Journal of Power Sources 195 (2010) 7583–7586

Contents lists available at ScienceDirect

Journal of Power Sources

journal homepage: www.elsevier.com/locate/jpowsour

Short communication

Preparation and performance of large-area $La_{0.9}Sr_{0.1}Ga_{0.8}Mg_{0.2}O_{3-\delta}$ electrolyte for intermediate temperature solid oxide fuel cell

Xiao-dong Zhu [a,b], Nai-qing Zhang [a], Li-jun Wu [a], Ke-ning Sun [a,*], Yi-xing Yuan [b]

[a] Academy of Fundamental and Interdisciplinary Sciences, Harbin Institute of Technology, Harbin, Heilongjiang 150080, China
[b] Center for Post-doctoral Studies of Civil Engineering, Harbin Institute of Technology, Harbin, Heilongjiang 150001, China

ARTICLE INFO

Article history:
Received 1 April 2010
Received in revised form 28 May 2010
Accepted 31 May 2010
Available online 8 June 2010

Keywords:
Solid oxide fuel cell
$La_{0.9}Sr_{0.1}Ga_{0.8}Mg_{0.2}O_{3-\delta}$
Large-area
Tape casting
Solid-state reaction method

ABSTRACT

Pre-treated LSGM starting powders decrease in particle size, leading to an increase in the LSGM relative density and electric conductivity. The starting powders are ball-milled with the assistance of absolute ethanol to reduce the particle size, dried ultrasonically to prevent the agglomeration of the powders and pre-calcined and re-balled to increase the rate of grain growth. These improvements make it possible to obtain single phase LSGM powders with small particle size at the calcination temperature of 1300 °C. A large-area (9 cm × 9 cm) LSGM electrolyte substrate has been prepared successfully by tape casting from these powders. The LSGM electrolyte exhibits a dense structure, the relative density reaches 96%, and the electrical conductivity is 0.08 S cm^{-1} at 800 °C.

1. Introduction

Solid oxide fuel cells (SOFCs) are promising energy conversion devices that can generate electric power through electrochemical reactions between an oxidant and a fuel gas [1]. Lowering the operating temperature of the SOFCs can significantly reduce the cost within the scope of interconnection, manifold and sealing materials [2]. One important approach is the application of an alternative electrolyte material such as La(Sr)Ga(Mg)$O_{3-\delta}$ [3], which has higher ionic conductivity than that of YSZ. $La_{0.9}Sr_{0.1}Ga_{0.8}Mg_{0.2}O_{3-\delta}$ (LSGM) has been identified as a superior oxide-ion electrolyte for medium- and low-temperature SOFCs because it possesses high chemical stability and negligible electronic conductivity over a wide range of oxygen partial pressures (1–10^{-20} atm) [4,5]. In our previous study, the LSGM electrolyte and electrodes with high electrochemical performance (SCF-LDC gradient cathodes and NiO–LDC composite anodes with LDC as the interlayer) were developed for LSGM-based SOFCs by means of optimizing their structures [6–8].

Tape casting is a well-known shaping technique to produce large-area, thin and flat ceramic tapes that are difficult to achieve via other methods such as pressing and extruding [9]. Because it is also potentially cost-effective for mass production, tape casting is an attractive technique to produce the SOFC components [10,11]. Unfortunately, the high sintering temperatures (above 1525 °C) cause the evaporation of Ga [12]. In our previous study, the relative density of LSGM was only 91% when it was sintered at 1500 °C because of the large particle size of LSGM powders prepared by the solid-state reaction method without pre-treating [6]. In this paper, the LSGM starting powders were pre-treated to reduce their particle size, to improve the sintering activity and to decrease the sintering temperatures. The relative density of the electrolyte reached 96% when it was sintered at 1500 °C, and a large-area (9 cm × 9 cm) LSGM electrolyte was obtained successfully by tape casting.

2. Experimental

2.1. Preparation of LSGM powders

The $La_{0.9}Sr_{0.1}Ga_{0.8}Mg_{0.2}O_{3-\delta}$ (LSGM) for the electrolyte was prepared from stoichiometric amounts of La_2O_3 (99.95%), $SrCO_3$ (99.9%), Ga_2O_3 (99.99%) and MgO (99.99%) by the solid-state reaction method. Before being weighed, La_2O_3, and MgO were heat treated at 1000 °C for 6 h in order to achieve decarbonation, while Ga_2O_3 and $SrCO_3$ were heat treated at 80 °C for 6h for dehydration. Each starting material was ball-milled with the aid of absolute ethanol for 24 h and dried ultrasonically. Then, these powders were mixed in stoichiometric amounts with an appropriate amount of absolute ethanol in a planetary ball mill, and milled for 24 h. The raw materials were dried at room temperature ultrasonically. Then the raw materials directly calcined at 1300 °C for 18 or 36 h to achieve the LSGM-A powders, denoted as LSGM-A18 or LSGM-A36.

* Corresponding author. Tel.: +86 451 86412153; fax: +86 451 86412153.
E-mail address: keningsun@yahoo.com.cn (K.-n. Sun).

0378-7753/$ – see front matter © 2010 Elsevier B.V. All rights reserved.
doi:10.1016/j.jpowsour.2010.05.060

The other raw materials were pre-calcined at 900 °C for 24 h and then calcined at 1300 °C for 18 or 36 h to obtain LSGM-B powders, denoted as LSGM-B18 or LSGM-B36. The raw powders were dry milled for 8 h, then pre-calcined at 1250 °C for 24 h and finally calcined at 1500 °C for 36 h in air to obtain LSGM powders that were denoted as LSGM-C [6].

2.2. Preparation of LSGM electrolyte

The LSGM-B36 was mixed with a solvent (butanone and ethanol), a dispersant (triethanolamine), plasticizers (polyethylene glycol and diethyl phthalate), and a binder (polyvinylbutyl). After being mixed and homogenized, the slurry was degassed using a vacuum pump and cast onto the surface of polyethylene films via a "doctor-blade" method. The cast tapes were dried at room temperature for 24 h and then sintered in air at 1500 °C for 6 h.

2.3. Material characterization

LSGM ceramics were Ø20 mm in diameter and 600–700 μm in thickness, and both sides were pasted with Pt with dimensions of 5 mm × 5 mm. The electrochemical impedance spectroscopy (EIS) test was conducted with a Princeton Applied PARSTAT 2273 impedance analyzer at the open circuit condition with a frequency range of 0.01–100 kHz. Scanning electron microscopy (SEM) was used to observe the microstructures with a Hitachi S4700. The particle size distribution of LSGM powders was tested with an LS-900 particulate size description analyzer. The porosity was measured by the Archimedes method. The phase of LSGM was examined with a Rigaku D/max-ΠB X-ray diffractometer (XRD) using Cu Kα radiation.

3. Results and discussion

Fig. 1 shows the X-ray diffraction patterns of the powders. The XRD pattern of the LSGM-C powder in Fig. 1 demonstrates that the LSGM powder calcined at 1500 °C for 36 h only consists of the single LSGM phase. The impurity phases such as $LaSrGaO_4$ or $LaSrGa_3O_7$, often created in the solid-state reaction method, did not appear in the sample. However, the particle size parameter (D_{50}) of LSGM-C reached 24.0 μm, as shown in Fig. 2. The values of D_{50} indicate that 50% of the particles in the sample are smaller than this diameter. Obviously, such large particles have low sintering activity and are not beneficial for the densification of the LSGM electrolyte. Consequently, we modified the preparation technique by ball-milling each starting material with the assistance of absolute ethanol, drying the powders ultrasonically and reducing the calcined temperature of the LSGM powders.

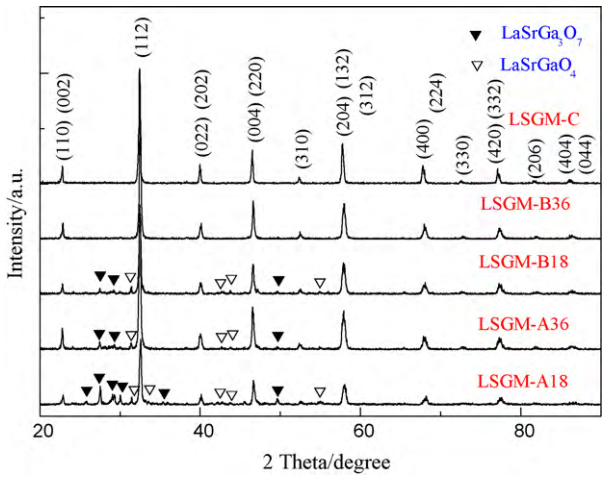

Fig. 1. XRD patterns of the LSGM powders prepared with different synthesis processes.

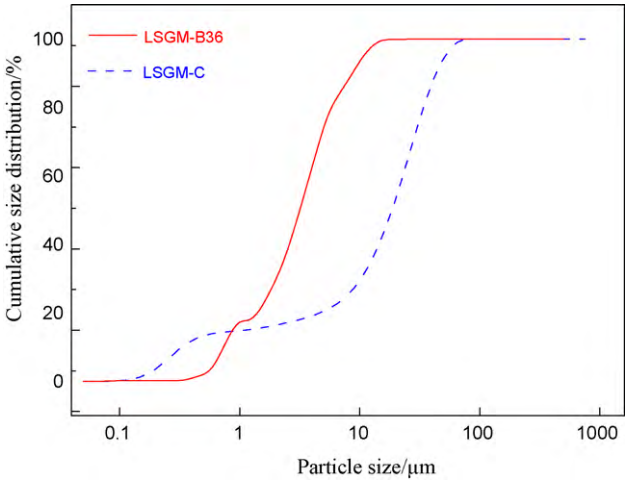

Fig. 2. Particle size distribution plots of the LSGM powders.

In Fig. 1, the XRD patterns of the powders of LSGM-A18 and LSGM-A36 show the LSGM, $LaSrGaO_4$ and $LaSrGa_3O_7$ phases. The single LSGM phase cannot be obtained at 1300 °C for either 18 or 36 h. A two-step calcination method was then tried. After pre-calcination at 900 °C for 24 h and re-balling, the XRD patterns show that LSGM-B18 still has impurities, but LSGM-B36 consists of only the single LSGM phase. This synthesis temperature is much lower than the results reported in the literature [6,13–15]. In addition, the D_{50} of LSGM-B36 is reduced to 3.0 μm, as shown in Fig. 2. The smaller the D_{50}, the finer the particles. It was demonstrated that LSGM-B36 was much finer than LSGM-C. This can be attributed to the following four reasons: (1) instead of the dry milling, the wet milling with the aid of absolute ethanol could prevent poor milling effects, resulting in powder adhesion onto the balls and the pot. (2) The D_{50} value of each starting material milled for 24 h decreased from 8–13 μm to 1–3 μm, and the homogeneity of the mixture was improved, resulting in more contact interfaces in the calcination process. (3) The ultrasonic drying restrained the agglomeration of powders due to the mechanical effects. (4) The pre-calcination and re-balling increased grain boundary diffusivity to accelerate the rate of grain growth.

All of the above reasons make it possible to obtain the single phase of LSGM at a synthesis temperature of 1300 °C and produce small particle sizes. Thus, it can be beneficial to the formation of the LSGM ceramic. Actually, some LSGM electrolyte substrates with LSGM-B36 as the active material, having a large-area (such as 5 cm × 5 cm, 9 cm × 9 cm, and 10 cm × 10 cm), with a thickness of 600–700 μm, were produced successfully by tape casting and sintering at 1500 °C. Fig. 3 shows a flat large-area (9 cm × 9 cm) LSGM disk. There are discolored spots on the brown substrate. These heterogeneous compositions may be the result of reactions with furnace dust or the setter plate.

Fig. 4 shows the surface and cross-sectional morphologies of the LSGM-B36 electrolyte. It can be seen that there are almost no open holes in the surface and interior, and the substrate appears fairly dense. The Archimedes method demonstrated that the density of LSGM-B36 reached 96% of the theoretical density, much higher than that of LSGM ceramic prepared with LSGM-C powders at the same sintering temperature [6].

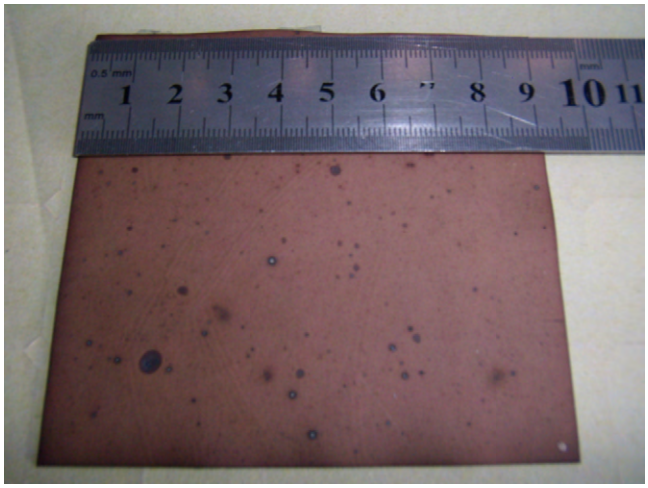

Fig. 3. Photograph of LSGM ceramic (9 cm × 9 cm).

The EIS measured from 350 to 800 °C and the equivalent circuits for the LSGM-B36 samples are shown in Fig. 5. It can be seen from Fig. 5 that the EIS measured at 350 °C is composed of a high frequency line {inductance (L)}, a high frequency arc {bulk resistance (R_b, Q_b)}, a low frequency arc {grain boundary resistance (R_g, Q_g)} and a low frequency line {electrode resistance (R_e, Q_e)}. The EIS measured at 450 °C consists of a depressed semicircle and a line. The semicircle and the line are related to (R_b, Q_b) plus (R_g, Q_g) and (R_e, Q_e), respectively. With the increase of the temperature, the semicircle becomes small until it fully disappears; the line becomes one arc at 800 °C, demonstrating that ion and electron transfer at the interface between the electrolyte and the electrodes appear much more easily. The electric conductivity of LSGM-B36 is 0.08 S cm^{-1} at 800 °C. Although this value is lower than that of LSGM prepared by the dry-pressing method [16], due to the relatively lower density of LSGM prepared by tape casting, it is twice as much as the electric conductivity of the electrolyte ceramics prepared using LSGM-C [6]. If the LSGM green tape is isostatically cold pressed before sintering, or if other sintering aids are added, then the relative density and the electric conductivity of LSGM will be further improved. This work is currently under way in our laboratory.

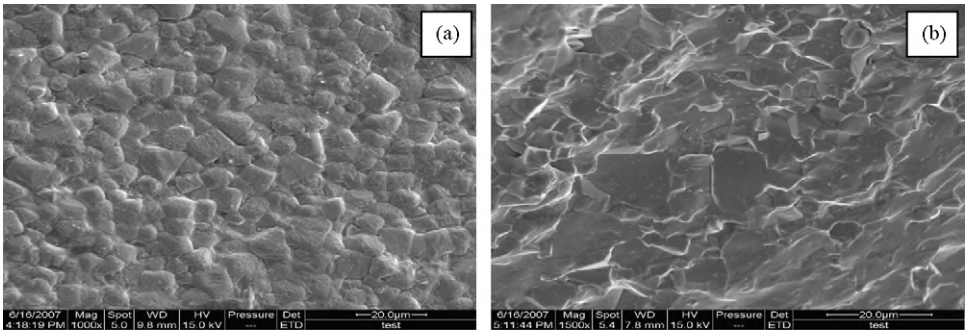

Fig. 4. SEM images of LSGM substrate: (a) surface and (b) cross-sectional.

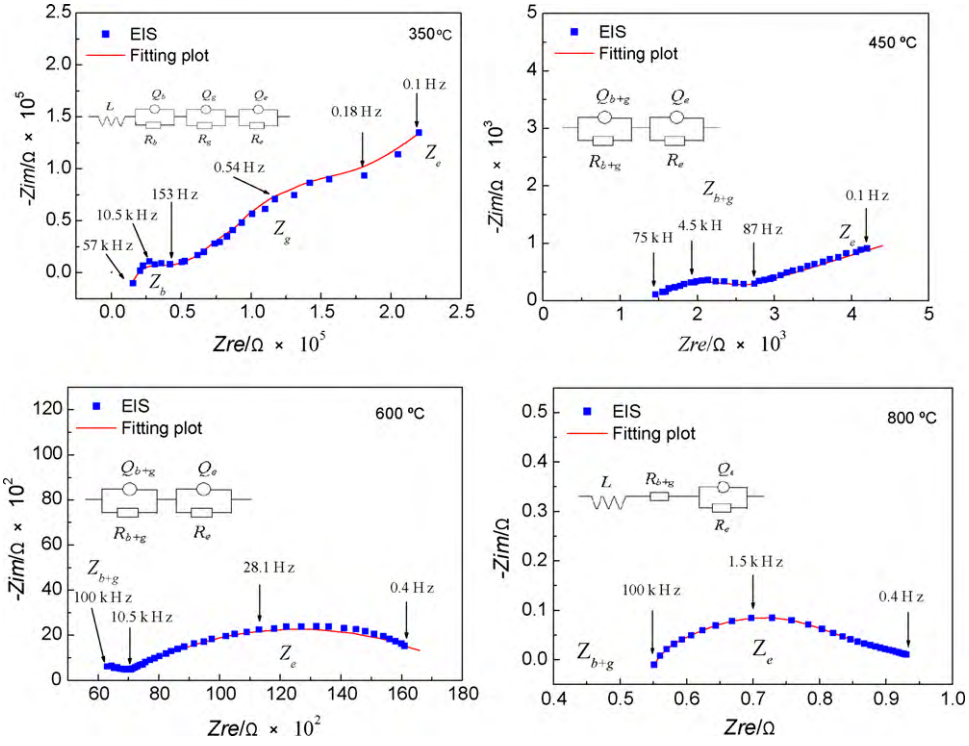

Fig. 5. Nyquist plots and equivalent circuits of LSGM ceramics measured at different temperatures.

4. Conclusions

A large-area LSGM electrolyte was prepared by tape casting. The LSGM substrate prepared with LSGM-B36 powder exhibited a dense structure with a relative density of about 96% and an electric conductivity of 0.08 S cm^{-1} at 800 °C. These properties were obtained by optimizing the solid-state reaction synthesis processes of the LSGM powders with the following improvements. (1) Instead of dry milling, wet milling with the aid of absolute ethanol can prevent poor milling results. (2) The starting materials with smaller particle size that were milled, pre-calcined and re-balled increased grain boundary diffusivity to accelerate the rate of grain growth. (3) The ultrasonic drying restrains the agglomeration of powders due to the mechanical effects. These reasons make it possible to obtain the single LSGM phase at a sintering temperature of 1300 °C and produce small particle sizes. With the active material, some LSGM-B36 electrolyte substrates with an area of about 9 cm × 9 cm and a thickness of 600–700 μm were produced successfully.

Acknowledgments

This project was financially supported by the Natural Scientific Research Innovation Foundation in Harbin Institute of Technology (No. HIT.NSRIF. 2008. 22), the International Cooperation Project of Science and technology (No. 2006DFA52660), the Provincial Nature Science Foundation of Heilongjiang (No. ZJG0703), and the China Postdoctoral Science Foundation (Nos. 20080430134 and 200902384).

References

[1] E.P. Murray, T. Tsai, S.A. Barnett, Nature 400 (1999) 649–651.
[2] S.C. Singhal, K. Kendall, High Temperature Solid Oxide Fuel Cells: Fundamentals, Design, and Applications, Elsevier, 2003.
[3] B.C.H. Steele, A. Heinzel, Nature 414 (2001) 345–352.
[4] T.I. Shihara, H. Matsuda, Y. Tskita, J. Am. Chem. Soc. 116 (1994) 3801–3803.
[5] M. Feng, J.B. Goodenough, Eur. J. Solid State Inorg. Chem. 31 (1994) 663–672.
[6] N.Q. Zhang, K.N. Sun, D.R. Zhou, D.C. Jia, J. Rare Earth 24 (2006) 90–92.
[7] X.D. Zhu, K.N. Sun, N.Q. Zhang, X.B. Chen, L.J. Wu, D.C. Jia, Electrochem. Commun. 9 (2007) 431–435.
[8] X.D. Zhu, K.N. Sun, S.R. Le, N.Q. Zhang, Q. Fu, X.B. Chen, Y.X. Yuan, Electrochim. Acta 54 (2008) 862–867.
[9] H. Moon, S.D. Kim, S.H. Hyun, H.S. Kim, Int. J. Hydrogen Energy 33 (2008) 1758–1768.
[10] C.J. Fu, S.H. Chan, Q.L. Liu, X.M. Ge, G. Pasciak, Int. J. Hydrogen Energy 35 (2010) 301–307.
[11] Y.J. Leng, S.H. Chan, K.A. Khor, S.P. Jiang, Int. J. Hydrogen Energy 29 (2004) 1025–1033.
[12] M. Peter, M. Thorsten, Int. J. Appl. Ceram. Technol. 6 (2009) 249–256.
[13] M. Shi, N. Liu, Y.D. Xu, C. Wang, Y.P. Yuan, P. Majewski, F. Aldinger, J. Mater. Process. Technol. 169 (2005) 179–183.
[14] B. Huang, X.J. Zhu, W.Q. Hu, Q.C. Yu, H.Y. Tu, J. Power Sources 186 (2009) 29–36.
[15] J. Peñna-Martínez, D. Marrero-López, J.C. Ruiz-Morales, B.E. Buergler, P. Núñez, L.J. Gauckler, J. Power Source 159 (2006) 914–921.
[16] T. Ishihara, H. Matsuda, Y. Takita, J. Am. Chem. Soc. 116 (1994) 3801.